

Microstructure of Al contacts on GaAs

I. Karpov, A. Franciosi, C. Taylor, J. Roberts, and W. L. Gladfelter

Citation: *Applied Physics Letters* **71**, 3090 (1997); doi: 10.1063/1.120255

View online: <http://dx.doi.org/10.1063/1.120255>

View Table of Contents: <http://scitation.aip.org/content/aip/journal/apl/71/21?ver=pdfcov>

Published by the [AIP Publishing](#)

Articles you may be interested in

[Microstructure of Ti/Al/Ni/Au ohmic contacts for N-polar GaN/AlGaN high electron mobility transistor devices](#)
J. Vac. Sci. Technol. B **32**, 011201 (2014); 10.1116/1.4829878

[Correlation between microstructure and temperature dependent electrical behavior of annealed Ti/Al/Ni/Au Ohmic contacts to AlGaIn/GaN heterostructures](#)
Appl. Phys. Lett. **103**, 201604 (2013); 10.1063/1.4828839

[Effect of the Ti-underlayer microstructure on the texture of Al thin films](#)
J. Vac. Sci. Technol. B **19**, 856 (2001); 10.1116/1.1362681

[Microstructural analysis of Al interconnects in microprocessor devices using EFTEM](#)
AIP Conf. Proc. **491**, 255 (1999); 10.1063/1.59913

[Electromigration mass transport phenomena in Al thin-film conductors with bamboo microstructure](#)
AIP Conf. Proc. **418**, 39 (1998); 10.1063/1.54660

The advertisement features a red and white color scheme. On the left, text reads 'Confidently measure down to 0.01 fA and up to 10 PΩ' and 'Keysight B2980A Series Picoammeters/Electrometers'. A red button with white text says 'View video demo'. In the center is a photograph of the Keysight B2980A device. On the right is the Keysight Technologies logo, which includes a stylized red waveform and the text 'KEYSIGHT TECHNOLOGIES'.

Microstructure of Al contacts on GaAs

I. Karpov and A. Franciosi^{a)}

Department of Chemical Engineering and Materials Science, University of Minnesota, Minneapolis, Minnesota 55455, and Laboratorio Nazionale TASC-INFN, Area di Ricerca, Padriciano 99, I-34012 Trieste, Italy

C. Taylor, J. Roberts, and W. L. Gladfelter

Department of Chemistry, University of Minnesota, Minneapolis, Minnesota 55455

(Received 6 June 1997; accepted for publication 23 September 1997)

The microstructure of Al films deposited on GaAs(100) 2×4 surfaces through chemical vapor deposition from dimethylethylamine alane in the 100–160 °C temperature range exhibits a dominant (111) texture which is not encountered in evaporated films. Such a texture has been associated with enhanced electromigration resistance in related systems. Growth of (111)-oriented grains is observed when the deposition rate is limited by the surface reaction of the impinging precursor molecules, while at higher temperatures (160–400 °C) only the conventional texture is observed. © 1997 American Institute of Physics. [S0003-6951(97)01147-9]

Aluminum-based vias are widely used in modern integrated circuit (IC) technology, but are well known to be susceptible to failure by electromigration.¹ Some of the important microstructural variables affecting electromigration lifetime, i.e., the mean time to failure, are grain size, grain size distribution, and texture.^{1,2} For example, the presence of Al grains with (111) texture was found to increase the electromigration lifetime of metallizations fabricated on Si(100) wafers by evaporation or sputtering.²

In principle, Al nucleation and the resulting film microstructure might be affected by the specifics of the deposition process, but relatively little is known about microstructure evolution during evaporation or chemical vapor deposition (CVD) of metals on semiconductors. Among the precursors currently been considered^{3–8} for Al CVD, dimethylethylamine alane (DMEAA) may offer several advantages because of its nonpyrophoric character, high vapor pressure and low pyrolysis temperature.^{6–8}

We report here major differences in the microstructure of Al films deposited by evaporation and CVD from DMEAA on atomically clean GaAs(100) 2×4 surfaces.

We employed a multichamber ultrahigh vacuum (UHV) system (base pressure $p\sim 4\times 10^{-10}$ Torr) that includes a UHV-compatible CVD reactor with reflection high-energy electron diffraction (RHEED) capabilities, and an analysis chamber with an Auger electron spectrometer, to deposit the films in the 100–400 °C substrate temperature range and precursor partial pressures (p_D) in the 2×10^{-4} – 2×10^{-5} Torr range.^{8–10}

The GaAs substrates for Al deposition were prepared by molecular beam epitaxy (MBE). Si-doped, epitaxial GaAs(100) 2×4 layers 1 μm thick were grown at 580 °C by solid source MBE on GaAs(100) wafers and protected by a thick (~ 0.5 μm thick) amorphous As cap layer during transfer in air to the reactor chamber.⁹ The cap layer was thermally desorbed in-situ to produce a sharp 2×4 RHEED pattern prior to Al deposition.^{9,10} The sample holder temperature was monitored by means of an optical pyrom-

eter operating at a wavelength of 2.1 μm . The final GaAs(001) rms surface roughness (1.4–1.7 Å) was comparable to that of as-grown GaAs surfaces.⁹

The DMEAA precursor was synthesized using the procedure described elsewhere⁷ and admitted to the reactor through a leak valve after repeated freeze-pump-thaw cycles.^{8,10} The precursor partial pressure p_D was monitored by means of a nude ion gauge calibrated to take into account the ionization probability of DMEAA.⁸ The final Al film thickness was measured *ex situ* by means of a profilometer using a diluted HF etch to remove the film from selected areas of the substrate.

For comparison, evaporated Al films on GaAs(100) 2×4 substrates were also obtained using the same experimental system on the same type of substrates, for similar values of the substrate temperature and Al deposition rate (0.5–1.0 Å/s). We employed a BN crucible surrounded by a W resistor coil filled with 99.999 wt. % Al and determined the deposition rate using a quartz crystal thickness monitor.

The film microstructure was characterized by x-ray diffraction (XRD), atomic force microscopy (AFM), and scanning electron microscopy (SEM). We used a single-crystal Siemens D-500 diffractometer or a Rigaku D-Max B diffractometer with a pole figure attachment. For the pole figure measurements, the Rigaku diffractometer was set at a 2θ value of 38.5° to monitor reflections from Al {111} planes. The sample was simultaneously tilted and rotated to record diffracted x-ray intensities up to a maximum tilt angle of 80° using the Schultz reflection technique.¹¹

The AFM studies were performed in air, using a commercial instrument which included a cantilever with spring constant of 0.58 N/m and a scanner with a scan area of 125 $\mu\text{m}\times 125$ μm . The SEM studies were performed on cleaved {110} cross sections of the Al/GaAs complex, using an Hitachi S800 microscope operated at 20 kV.

Films deposited by CVD exhibited, in general, a columnar microstructure under cross-sectional SEM examination. The grain size distribution, as studied by AFM, had a single maximum. The average grain size increased with film thickness and was about 0.2–0.3 μm for 0.3–0.5 μm thick films deposited at 200 °C.

^{a)}Also with Dipartimento di Fisica, Università di Trieste, I-34127 Trieste, Italy.

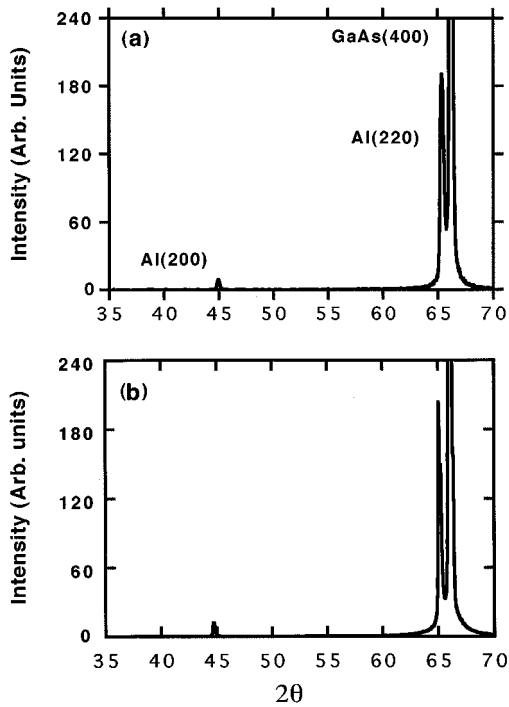


FIG. 1. X-ray diffraction patterns recorded from Al films fabricated by chemical vapor deposition (CVD) from (a) dimethylethylamine alane (DMEAA) and (b) evaporation 0.4 and 0.35 μm thick, respectively, deposited at $T_D=400^\circ\text{C}$ on GaAs(100) 2×4 surfaces.

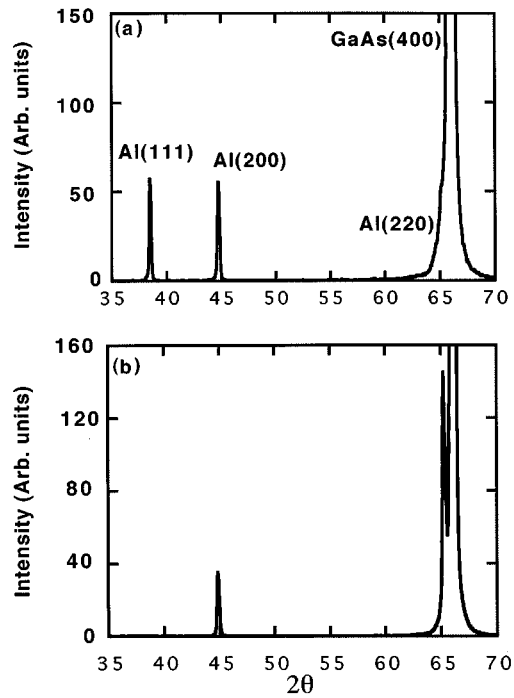


FIG. 2. X-ray diffraction patterns recorded from (a) CVD and (b) evaporated Al films 0.35 and 0.3 μm thick, respectively, deposited at $T_D=150^\circ\text{C}$ on GaAs(100) 2×4 surfaces. In addition to the Al(200) and Al(220) reflections, the latter visible only as a shoulder on the left side of the GaAs(400) peak, Al films fabricated by CVD from DMEAA at 150°C exhibit an important Al(111) contribution.

Representative XRD patterns obtained from Al films grown by CVD from DMEAA and evaporation are shown in Fig. 1 for a deposition temperature $T_D=400^\circ\text{C}$ and in Fig. 2 for $T_D=150^\circ\text{C}$. The film thickness was 0.40 and 0.35 μm for CVD and evaporation, respectively, in Fig. 1, and 0.35 and 0.30 μm for CVD and evaporation, respectively, in Fig. 2. Comparison of Fig. 1 and Fig. 2 clearly indicates that while films produced by CVD and evaporation at 400°C exhibit virtually identical XRD patterns, there are substantial differences in the microstructure of films fabricated by CVD and evaporation at 150°C . The major Al-related peaks in Figs. 1(a) and 1(b) correspond to the Al(220) reflection, i.e., to Al crystallites with $\{110\}$ planes oriented parallel to the GaAs(100) substrate. A much weaker Al(200) reflection is also observed, suggesting the presence of at least some crystallites with $\{100\}$ planes parallel to GaAs(100) surface. The relative intensities and width of the diffraction peaks for the two films fabricated at 400°C are compellingly similar. The similarity of the two microstructures for films produced by CVD and evaporation at 400°C is also supported by $\{111\}$ pole figures (not shown), which reflect $\{111\}$ planes of Al crystallites arranged with $\{110\}$ plane parallel to the (100) substrate, and a dominant Al(011)[100]||GaAs(001) $\langle 110 \rangle$ epitaxial relation.

In addition to the Al(200) and Al(220) reflections, Al films fabricated by CVD from DMEAA at 150°C [see Fig. 2(a)] exhibited an important Al(111) contribution. The Al(111) reflection is instead completely absent from the XRD patterns recorded for Al films evaporated on GaAs(100) 2×4 at 150°C [see Fig. 2(b)], 400°C [see Fig. 1 (b)], or for that matter even at room temperature.¹² Al films fabricated by evaporation at 150°C , for example [see Fig.

2(b)], show only major Al-related peaks corresponding to the Al(220) and Al(200) reflections.

A more quantitative analysis was performed by recording a series of XRD patterns for films of similar thickness (0.3–0.5 μm) fabricated for different values of T_D , and monitoring the ratio of the integrated diffraction intensities of the Al(111) and Al(200) peaks. The results are shown in Fig. 3(a) as a function of the deposition temperature T_D . Our analysis show that little or no Al(111) contribution is observed for $T_D>160^\circ\text{C}$, while the same contribution increases rapidly with decreasing deposition temperature below 160°C . The same type of qualitative dependence on T_D , only magnified, would be observed in the Al(111)/Al(220) intensity ratio (not shown), since the Al(200)/Al(220) intensity ratio increases *per se* with decreasing deposition temperature.

A complete analysis of the film texture using pole figures reveals the presence of several minority domains with different orientations in addition to the major (111) textured component in films fabricated by CVD at low temperature. The main additional orientations were: (a) Al(100)[001]||GaAs(100)[001]; (b) Al(100)[001]||GaAs(100)[011]; (c) Al(110)[001]||GaAs(100)[011]; (d) Al(110)[001]||GaAs(100)[01 $\bar{1}$]. Orientation (a) above was also recently observed in Al films grown on GaAs(100) by chemical beam epitaxy from trimethylamine alane,¹³ while orientations (b)-(d) above have also been reported in previous studies of MBE grown Al films on GaAs(100).¹⁴

With increasing deposition temperature the main (111)-textured contribution becomes weak and for $T_D>300^\circ\text{C}$ a

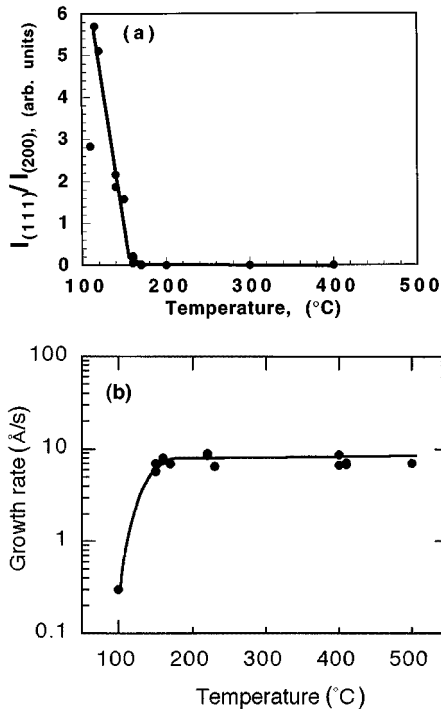


FIG. 3. (a) Ratio of Al(111) to Al(200) diffraction intensities for CVD films of similar thickness ($0.3\text{--}0.5\ \mu\text{m}$) deposited on GaAs(100) 2×4 surfaces as a function of the deposition temperature T_D . (b) Logarithmic growth rate for Al films fabricated by CVD from DMEAA on GaAs(100) 2×4 surfaces. We show results as a function of the substrate temperature T_D for a constant partial pressure of DMEAA $p_D=2\times 10^{-4}$ Torr. The growth rate is limited by the temperature-activated surface reaction rate only for $T_D < 150\text{--}160^\circ\text{C}$.

dominant Al(110)[001]||GaAs(100)[011] orientation is observed for both CVD and evaporation, yielding a completely analogous microstructure.

The results of Figs. 1–2 suggest that at low enough deposition temperatures, the specifics of the CVD process may start to affect the film microstructure. This suggestion is supported by a comparison of the results in Fig. 3(a) with the kinetics of the CVD process from DMEAA. In Fig. 3(b) we show (from Ref. 8) the measured Al growth rate on GaAs(100) 2×4 as a function of T_D in the $100\text{--}500^\circ\text{C}$ range, for a fixed value of $p_D=2\times 10^{-4}$ Torr. The results show that for $T_D > 160^\circ\text{C}$ the films grew at a similar rate of about $8\ \text{\AA}/\text{s}$, while for $T_D < 150\text{--}160^\circ\text{C}$ the growth rate decreased rapidly, dropping to about $0.3\ \text{\AA}/\text{s}$ for $T_D \sim 100^\circ\text{C}$, and hinting at an Arrhenius-type dependence of the growth rate. The growth rate was also found to be directly proportional to p_D for $T_D > 160^\circ\text{C}$ (not shown). Therefore for $T_D > 160^\circ\text{C}$ the deposition process is flux limited, while for $T_D < 150\text{--}160^\circ\text{C}$ the growth rate is limited by the surface reaction rate of the impinging precursor molecules.⁸

Since the Al(111) reflection has not been observed in XRD patterns from Al films evaporated at room temperature on GaAs(100)—see Fig. 2(b) and Ref. 12—while it has been detected in films evaporated at 0°C on the same surface,¹⁵ it would appear that a substantial decrease in the surface mobility of the Al atoms is required to favor the growth of Al(111) crystallites during evaporation. Al films evaporated at room temperature on amorphous or highly disordered materials such as glass,¹⁶ or polymers,¹⁷ also exhibit (111) tex-

ture, further suggesting that a reduced surface mobility might be the key to the nucleation of (111)-oriented Al crystallites.

We therefore correlate the appearance of an increasing (111) contribution in films fabricated by CVD at decreasing deposition temperatures below $150\text{--}160^\circ\text{C}$ with a reduction in the surface mobility of the Al adatoms. We tentatively associate such a reduction with the presence of an increasing number of precursor molecules or reaction by-products adsorbed nondissociatively onto the the surface, i.e., to an increase in the average residence time of the corresponding molecules. The decrease in the overall CVD rate for $T_D < 150\text{--}160^\circ\text{C}$ in Fig. 3(b) is a clear manifestation of a reduction in the surface reaction rate of the precursor molecules, and we suggest that the adsorbed molecules might compete with Al adatoms for the available surface sites and lead to an important reduction in surface diffusion.

This work was supported in part by NSF under Grant No. DMR-9525758. The authors thank Lucia Sorba for her invaluable help with the growth of the GaAs substrates and Kai-Ann Yang for the synthesis of the DMEAA precursor.

¹C. V. Thompson and J. R. Lloyd, *Mater. Res. Bull.* **11**, 19 (1993).

²S. Vaidya and A. K. Sinha, *Thin Solid Films* **75**, 253 (1981).

³T. J. Licata, E. G. Colgan, J. M. E. Harper, and S. E. Luce, *IBM J. Res. Dev.* **34**, 419 (1995).

⁴*The Chemistry of Metal CVD* edited by T. Kodas and M. H. Smith (VCH, Weinheim, 1994).

⁵H. H. Lee, *Fundamentals of Microelectronics Processing* (McGraw-Hill, New York, 1990); J.-H. Yun and S.-K. Park, *Jpn. J. Appl. Phys.* **34**, 3216 (1995).

⁶M. Simmonds and W. L. Gladfelter, in *The Chemistry of Metal CVD*, edited by T. Kodas and M. H. Smith (VCH, Weinheim, 1994), Chap. 2.

⁷M. G. Simmonds, E. C. Phillips, J. W. Hwang, and W. L. Gladfelter, *Chemtronics* **5**, 155 (1991).

⁸I. Karpov, W. Gladfelter, and A. Franciosi, *Appl. Phys. Lett.* **69**, 4191 (1996).

⁹Y. Fan, I. Karpov, G. Bratina, L. Sorba, W. Gladfelter, and A. Franciosi, *J. Vac. Sci. Technol. B* **14**, 623 (1996); I. Karpov, N. Venkateswaran, G. Bratina, W. Gladfelter, A. Franciosi, and L. Sorba, *ibid.* **13**, 2041 (1995).

¹⁰N. Venkateswaran, I. Karpov, W. Gladfelter, and A. Franciosi, *J. Vac. Sci. Technol. A* **14**, 1949 (1996); I. Karpov, G. Bratina, L. Sorba, A. Franciosi, M. G. Simmonds and W. L. Gladfelter, *J. Appl. Phys.* **76**, 3471 (1994).

¹¹B. D. Cullity, *Elements of X-ray Diffraction*, 2nd ed. (Addison-Wesley, Reading, MA, 1978), p. 297.

¹²J. Massies, P. Etienne, and N. T. Linh, *Surf. Sci.* **80**, 550 (1979); G. Landgren, R. Ludeke, and C. Serrano, *J. Cryst. Growth* **60**, 393 (1982); C. J. Kiely and D. Cherns, *Philos. Mag. A* **59**, 1 (1989); P. M. Petroff, L. C. Feldman, A. Y. Cho, and R. Williams, *J. Appl. Phys.* **52**, 7317 (1981).

¹³D. Sun, R. Beanland, T. B. F. Joyce, J. V. Armstrong, T. J. Bullough, and P. J. Goodhew, *J. Cryst. Growth* **132**, 592 (1993).

¹⁴P. N. Petroff, L. C. Feldman, A. Y. Cho, and R. S. Williams, *J. Appl. Phys.* **52**, 7317 (1981); R. Ludeke, and G. Landgren, *J. Vac. Sci. Technol.* **19**, 667 (1981); C. J. Kelly and D. Cherns, *Philos. Mag. A* **59**, 1 (1989).

¹⁵P. K. Bhattacharya, J. E. Oh, J. Singh, D. Biswas, R. Clarke, W. Dos Passos, R. Merlin, N. Mestres, K. H. Chang, and R. Gibala, *J. Appl. Phys.* **67**, 3700 (1990).

¹⁶G. Sberveglieri, V. Canevari, N. Romeo, and C. Spaggiari, *Mater. Res. Soc. Symp. Proc.* **54**, 675 (1986).

¹⁷R. J. De Angelis, R. J. Jacob, and J. E. Funk, *Thin Solid Films* **202**, 91 (1991); W. L. Gladfelter, D. C. Boyd, and K. F. Jensen, *Chem. Mater.* **1**, 339 (1989).